JOC*Article*

# Novel Fused D−A Dyad and A−D−A Triad Incorporating Tetrathiafulvalene and *p*-Benzoquinone

Frédéric Dumur, Nicolas Gautier, Nuria Gallego-Planas, Yücel Şahin,† Eric Levillain, Nicolas Mercier, and Piétrick Hudhomme*

*Ingénierie Moléculaire et Matériaux Organiques, UMR 6501, Boulevard Lavoisier, Université d'Angers, F-49045 Angers, France*

Matteo Masino and Alberto Girlando

*Dipartimento Chimica Generale ed Inorganica, Chimica Analitica, Chimica Fisica, Università di Parma, Parco Area delle Scienze, I-43100, Parma, Italy*

Vega Lloveras, José Vidal-Gancedo, Jaume Veciana, and Concepció Rovira

*Institut de Ciència de Materials de Barcelona (C.S.I.C), Campus de la U.A.B, 08193 Bellaterra, Spain*

*pietrick.hudhomme@univ-angers.fr*

*Received November 17, 2003*

Novel fused donor−acceptor dyad (TTF−Q or D−A) and acceptor−donor−acceptor triad (Q−TTF−Q or A−D−A) incorporating the donor tetrathiafulvalene (TTF) and the acceptor *p*-benzoquinone (Q) have been synthesized. The solution UV−vis spectra of these molecules display a low-energy absorption band that is attributed to an intramolecular charge transfer between both antagonistic units. The presence of reversible oxidation and reduction waves for the donor and acceptor moieties was shown by cyclic voltammetry, in agreement with the ratio TTF/quinone(s) units. The successive generation from these compounds of the cation radical and anion radical obtained upon (electro)-chemical oxidation and reduction, respectively, was monitored by optical and ESR spectroscopies. The anion radical $Q-TTF-Q^{-\bullet}$ triad was demonstrated to be a class II mixed-valence system with the existence of a temperature-dependent intramolecular electron transfer. The crystallographic tendency of these fused systems to overlap in mixed stacks of alternating A−D−A units is also discussed.

## Introduction

Much attention is still devoted to the investigation of D−A dyads and D−A−D and A−D−A triads in order to control the stoichiometry of both donor (D) and acceptor (A) partners, as well as the degree of charge transfer, which are crucial parameters in the design of organic metals. This considerable research effort is justified by the potential applications of these molecular systems, which are the basis for artificial photosynthetic systems,[1] materials presenting semiconducting or nonlinear optical properties,[2] molecular electronic,[3] and photovoltaic[4] devices. Development of new donor−acceptor architectures affording highly polarizable molecules is particularly important in order to progress in these fields. These compounds are characterized by low excitation energies leading to interesting optical properties. These could also be candidates for single one-component conductors showing intrinsic conductivities when relative donating and accepting abilities are controlled.[5] Moreover, the challenge of verifying experimentally the Aviram−Ratner concept of unimolecular electrical rectification on D−$\sigma$−A system,[6] in which the donor tetrathiafulvalene (TTF) and the acceptor tetracyanoquinodimethane (TCNQ) are connected via a saturated link, was recently achieved on the D−$\pi$−A hexadecylquinolinium tricyanoquinodimethanide molecule: the excited neutral state was found to be relatively accessible from the zwitterionic ground state $D^{+}-\pi-A^{-}$.[7] Tetrathiafulvalene has attracted much interest for its high electron-donating ability in this field of intramolecular charge-transfer materials.[8] But, to avoid the major problem in the synthesis of TTF−spacer−acceptor compounds resulting in the formation of the

* Corresponding author. Fax: +33 2 41 73 54 05.
† Permananent address: Department of Chemistry, Anadolu University, T-26470 Eskişehir, Turkey.

(1) (a) Fox, M. A., Chanon, M., Eds.; *Photoinduced Electron Transfer*; Elsevier: Amsterdam, 1988. (b) Kurreck, H.; Huber M. *Angew. Chem., Int. Ed. Engl.* **1995**, *34*, 849.

(2) (a) Prasad, P. N.; Williams, D. J. *Introduction to Nonlinear Optical Effects in Molecules and Polymers*; Wiley: New York, 1991. (b) Nalwa, H. S. *Adv. Mater.* **1993**, *5*, 341. (c) Long, N. J. *Angew. Chem., Int. Ed. Engl.* **1995**, *34*, 21. (d) Wong, M. S.; Bosshard, C.; Pan, F.; Günter, P. *Adv. Mater.* **1996**, *8*, 677.

(3) (a) Metzger, R. M.; Panetta, C. *New. J. Chem.* **1991**, *15*, 209. (b) Launay J. P. *Molecular Electronics. In Granular Nanoelectronics*; Ferry, D. K., Ed.; Plenum Press: New York, 1991. (c) Petty, M. C., Bryce, M. R., Bloor, D., Eds.; *Introduction to Molecular Electronics*; Oxford University Press: New York, 1995.

(4) Martín, N.; Sánchez, L.; Illescas, B.; Pérez I. *Chem. Rev.* **1998**, *98*, 2527.

(5) Yamashita, Y.; Tomura, M. *J. Mater. Chem.* **1998**, *8*, 1933.

(6) Aviram, A.; Ratner M. *Chem. Phys. Lett.* **1974**, *29*, 277.

10.1021/jo035689f CCC: $27.50 
Published on Web 02/21/2004

**CHART 1**

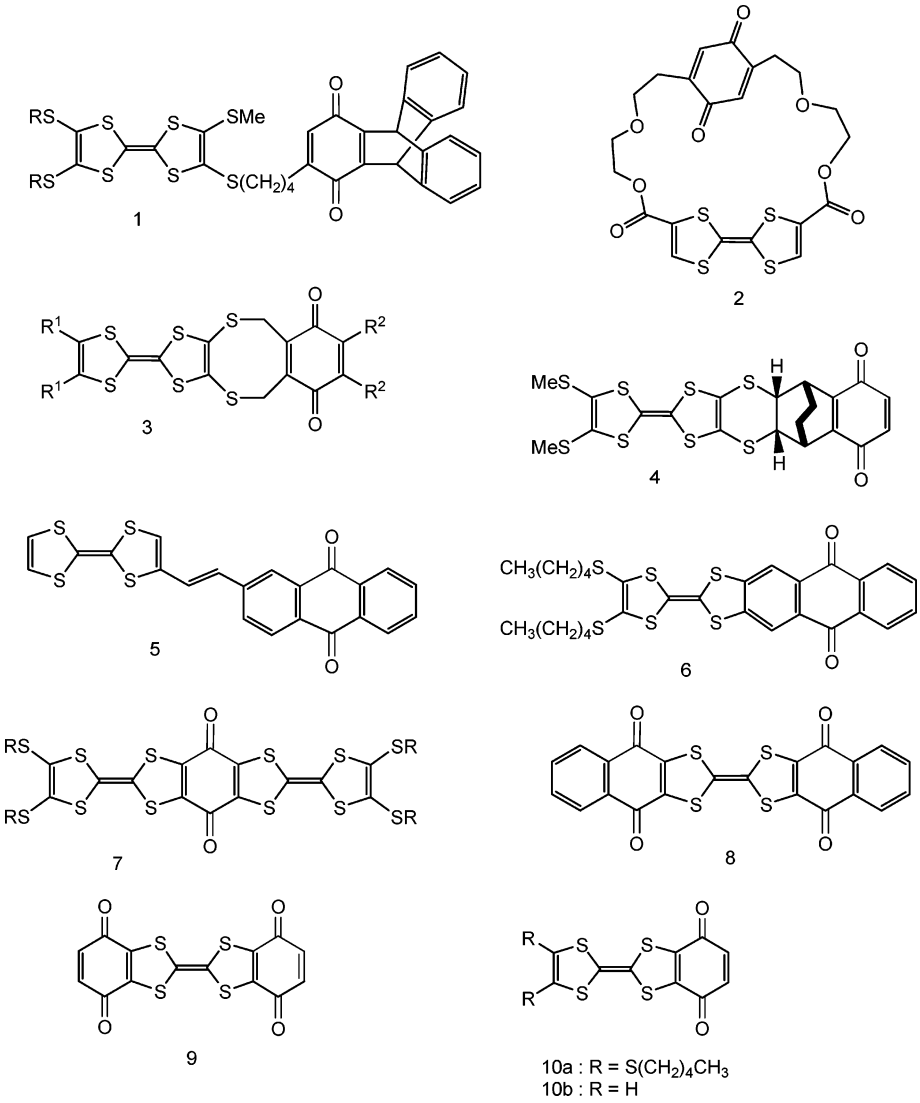


stable and insoluble intermolecular charge-transfer complex between both counterparts prior to their covalent linking, an alternative route was developed considering the linkage of the TTF derivatives to a weak electron acceptor such as quinone. The subsequent conversion into the strong TCNQ acceptor was investigated, but despite several attempts, there appears to be no example of a TTF−quinone being converted into the corresponding TTF−TCNQ derivative.

Several TTF−$\sigma$−quinone dyads were previously studied, but no intramolecular charge-transfer band was discernible in the UV−visible spectrum for molecules **1**,[9] **2**,[10] and **3**[11] (Chart 1). Molecule **4**, with a design having a fixed distance and orientation between the TTF and the quinone moieties, showed a weak intramolecular charge-transfer interaction.[12] The molecular type of conjugated **5**[13] or fused **6**[14] D−A dyads with anthraquinone as the acceptor, as well as fused D−A−D **7**[15] and A−D−A **8**[16] triads, were also introduced. In this latter case, the poor solubility of triad **8** prevented a further functionalization and also the structural study of this A−D−A system. Additionally and very surprisingly, the

(7) (a) Metzger, R. M.; Chen, B.; Höpfner, U.; Lakshmikantham, M. V.; Vuillaume, D.; Kawai, T.; Wu, X.; Tachibanan, H.; Hughes, T. V.; Sakurai, H.; Hosch, C.; Cava, M. P.; Brehmer, L.; Ashwell, G. J. *J. Am. Chem. Soc.* **1997**, *119*, 10455. (b) Metzger, R. M. *J. Mater. Chem.* **1999**, *9*, 2027. (c) Metzger, R. M. *Acc. Chem. Res.* **1999**, *32*, 950. (d) Roth, S.; Blumentritt, S.; Burghard, M.; Cammi, E.; Carroll, D.; Curran, S.; Düsberg, G.; Liu, K.; Muster, J.; Philipp, G.; Rabenau, T. *Synth. Met.* **1998**, *94*, 105. (e) Metzger, R. M. *Chem. Rev.* **2003**, *103*, 3803.

(8) (a) Segura, J. L.; Martín, N. *Angew. Chem., Int. Ed.* **2001**, *40*, 1372. (b) Bryce, M. R. *J. Mater. Chem.* **2000**, *10*, 589. (c) Bryce, J. M. *Adv. Mater.* **1999**, *11*, 11.

(9) Scheib, S.; Cava, M. P.; Baldwin, J. W.; Metzger, R. M. *J. Org. Chem.* **1998**, *63*, 1198.

(10) Moriarty, R. M.; Tao, A.; Gilardi, R.; Song, Z.; Tuladhar, S. M. *Chem. Commun.* **1998**, 157.

(11) (a) Segura, J. L.; Martín, N.; Seoane, C.; Hanack, M. *Tetrahedron. Lett.* **1996**, *37*, 2503. (b) Gonzales, M.; Illescas, B.; Martín, N.; Segura, J. L.; Seoane, C.; Hanack, M. *Tetrahedron* **1998**, *54*, 2853.

(12) Tsiperman, E.; Regev, T.; Becker, J. Y.; Bernstein, J.; Ellern, A.; Khodorkovsky, V.; Shames, A.; Shapiro, L. *Chem. Commun.* **1999**, 1125.

(13) Pérez, I.; Liu, S.-G.; Martín, N.; Echegoyen, L. *J. Org. Chem.* **2000**, *65*, 3796.

(14) Gautier, N.; Mercier, N.; Riou, A.; Gorgues, A.; Hudhomme, P. *Tetrahedron Lett.* **1999**, *40*, 5997.

(15) (a) Adam, M.; Müllen, K. *Adv. Mater.* **1994**, *6*, 439. (b) Frenzel, S.; Müllen, K. *Synth. Met.* **1996**, 175.

(16) (a) Watson, W. H.; Eduok, E. E.; Kashyap, R. P.; Krawiec, M. *Tetrahedron* **1993**, *49*, 3035. (b) The bis(1,4-naphthoquinone)TTF exhibited a reduction wave at $E°_{1/2} = -0.32$ V (NHE), but at both negative and positive potentials, the current increases sharply with increasing voltage, giving no distinct oxidation−reduction couples.

**SCHEME 1**[a]

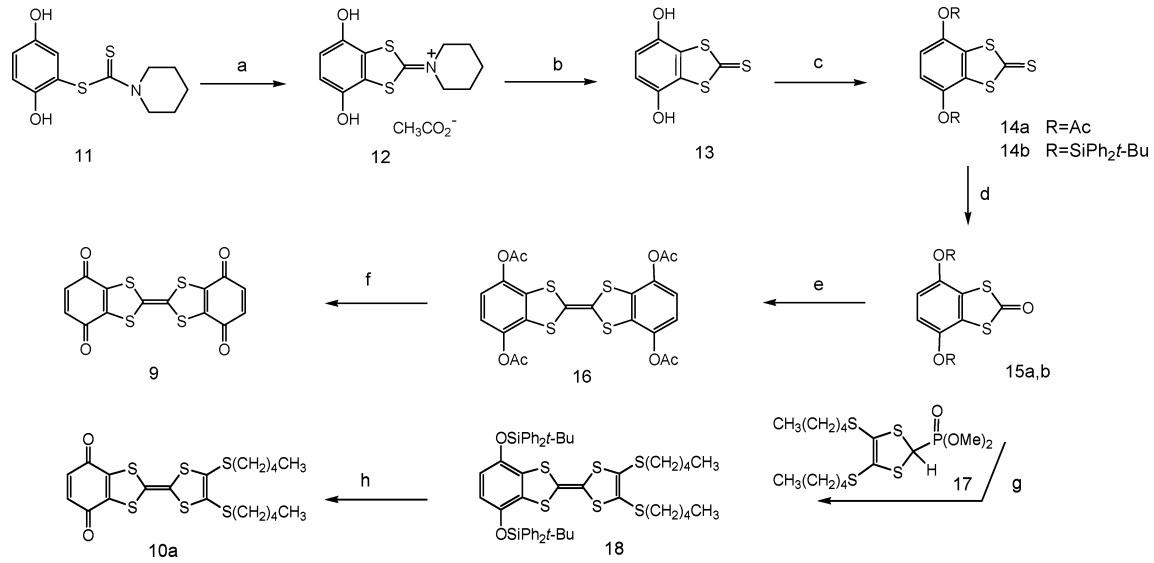


[a] Reagents: (a) *p*-benzoquinone then glacial AcOH, 80 °C, 96% (lit.[19a] 63%). (b) $Na_2S{\cdot}9H_2O$, MeOH, 98% (lit.[19a] 71%). (c) $Ac_2O$, $Et_3N$, 80% for **14a**; $Ph_2tBuSiCl$, DMF, imidazole, 86% for **14b**. (d) $Hg(OAc)_2$, $CH_2Cl_2$/glacial AcOH, 88% for **15a**, 85% for **15b**. (e) Δ $P(OEt)_3$, 45% (lit.[19a] 47% using $P(OEt)_3$/toluene). (f) (i) MeONa/MeOH; (ii) PTSA, $H_2O$; (iii) DDQ, 57%. (g) phosphonate **17**, *n*-BuLi, THF, −78 to 20 °C, 90%. (h) (i) *n*-$Bu_4NF$/THF; (ii) *p*-benzoquinone, 75%.

cyclic voltammetry study did not exhibit the oxidation waves corresponding to the TTF donor fragment.[16] On the other hand, the cyclic voltammetry of compound **7** revealed the presence of two two-electron oxidation waves corresponding to both TTF moieties, but no data were reported on the electrochemical behavior of the *p*-benzoquinone fragment.[15]

In this work we report the synthesis, theoretical calculations, spectroscopic and electrochemical properties of A−D−A triad **9** (Q−TTF−Q) and D−A (TTF−Q) dyad **10** corresponding to fused TTF−quinone(s) assemblies, also considered to be potential precursors for fused donor−acceptor oligomers or TTF−TCNQ systems. The study of the derived oxidized and reduced species is also presented in which previous results demonstrated that intramolecular electron transfer (IET) process occurred in the mixed-valence $Q-TTF-Q^{-\bullet}$ system.[17] Moreover, we present the study of the crystallographic arrangement of the fused Q−TTF−Q **9** to check if the previously proposed concept of designing organic metals with A−D−A type molecules, where the donors and acceptors are covalently linked via a saturated methylene spacer or a sulfur atom,[18] can be extended to fused systems.

## Results and Discussion

**Synthesis.** The synthesis of triad A−D−A **9** and dyad D−A **10** was performed using the same key intermediate 2-oxo-1,3-dithiole derivative **15** (Scheme 1). *p*-Benzoquinone was reacted with the dithiocarbamate salt (isolated from the addition of piperidine to carbon disulfide) in the presence of glacial acetic acid in a mixture of DMF/DMSO as solvents. The corresponding Michael addition followed by the aromatization produced compound **11** in 97% yield. The latter was further oxidized using *p*-benzoquinone, and the following cyclization upon treatment with glacial acetic acid led to the iminium salt **12** in 96% yield for the two steps.[19] After quantitative conversion to the corresponding 2-thioxo-1,3-dithiole **13** using sodium sulfide, the hydroquinone functionalities were protected using the acetyl or silyl groups. Well-established procedures afforded compounds **14a** and **14b** in 80 and 86% yields, respectively. The transchalcogenation upon treatment with mercuric acetate furnished the 2-oxo-1,3-dithiole derivatives **15** in excellent yields.

The triethyl phosphite coupling methodology was applied to **15a**, and the resulting tetrathiafulvalene **16** was isolated as yellow crystals in 45% yield. Subsequent methanolysis using a methoxide solution in THF/MeOH afforded TTF−bis(1,4-hydroquinone) after treatment with *p*-toluenesulfonic acid (PTSA).[20] Without isolating the fused TTF−bis(1,4-hydroquinone) intermediate, the oxidation was carried out using DDQ to yield the fused A−D−A system **9** as green-blue crystals after classical workup and chromatography on florisil using $CH_2Cl_2$/EtOAc (99/1) as the mixture of eluents.

To reach the fused D−A assembly **10a**, we applied a nonclassical Horner−Wadsworth−Emmons olefination to create the TTF core involving the 2-oxo-1,3-dithiole functionality.[21] After reaction of **15b** with the anion of phosphonate **17**[22] in THF and silicagel column chroma-

(17) Some parts of this work have been previously reported: Gautier, N., Dumur, F.; Lloveras, V.; Vidal-Gancedo, J.; Veciana, J.; Rovira, C.; Hudhomme, P. *Angew. Chem., Int. Ed.* **2003**, *42*, 2765.

(18) Khodorkovsky, V.; Becker J. Y. *Organic Conductors, Fundamentals and Applications*; Farges, J. P., Ed.; New York, 1994.

(19) (a) Synthesis of this compound was carried out according to a previously described methodology, several yields being improved by small modifications of experimental procedures: Sun, D.; Krawiec, M.; Watson, W. H. *J. Chem. Crystallogr.* **1997**, *27*, 515. (b) Yields were particularly improved by using piperidine instead of pyrrolidine: Gautier, N.; Gallego-Planas, N.; Mercier, N.; Levillain, E.; Hudhomme, P. *Org. Lett.* **2002**, *4*, 961.

(20) We should note that an identical reaction using inorganic acids such as hydrochloric acid or sulfuric acid solutions was unsuccessful. In these cases, the resulting precipitate could be the result of concomitant protonation of the TTF core.

(21) Boulle, C.; Desmars, O.; Gautier, N.; Hudhomme, P.; Cariou, M.; Gorgues, A. *Chem. Commun.* **1998**, 2197.

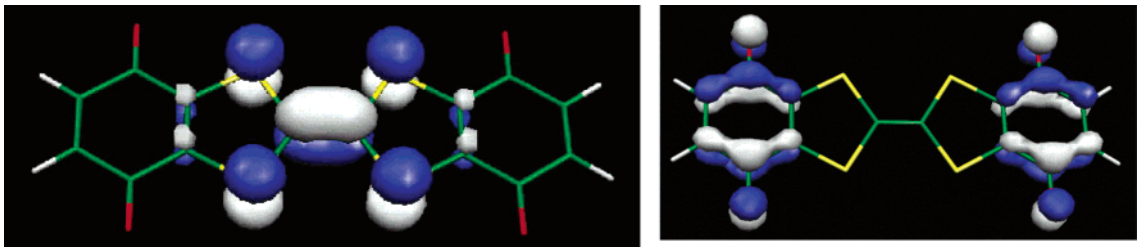

**FIGURE 1.** HOMO orbital (left) and LUMO orbital (right) of triad **9** obtained by DFT calculations.

tography ($CH_2Cl_2$/petroleum ether (1/4) as the mixture of eluents), we could isolate compound **18** as yellow crystals in 90% yield. The deprotection of the silyl group was carried out using tetrabutylammonium fluoride, and then subsequent oxidation using *p*-benzoquinone afforded compound **10a** as green crystals in 75% yield after column chromatography on florisil using $CH_2Cl_2$/petroleum ether (1/1) as the mixture of eluents.

**Theoretical Calculations and Spectroscopic Properties of 9 and 10.** Density Functional Theory (DFT) calculations were performed using Gaussian 98[23] at the B3LYP/6-31G* level of theory for a full geometry optimization, with no symmetry contraints, of the fused D−A and A−D−A systems. Even if no symmetry was imposed, the optimized geometry obtained confirmed the high symmetry of this A−D−A molecule ($D_{2h}$ symmetry). For the A−D−A assembly **9**, the molecular orbital analysis of both compounds showed that the largest coefficients in the HOMO orbital are mainly located on the central TTF core (the $S_2C{=}CS_2$ fragment) and the calculated energy value for this HOMO orbital was −5.35 eV (Figure 1). As expected, the coefficients in the LUMO orbital were centered on the quinone moieties, showing an alternation of $\pi$-bond signs in these rings, but this LUMO orbital was characterized by two quasi-degenerated orbitals: the LUMO (−3.89 eV) and the LUMO +1 (−3.84 eV). Consequently, the calculated HOMO−LUMO gap was estimated to be 1.46 eV. The degenerated LUMO orbital is due to alternating signs of the wave function coefficients in the $\pi$-molecular orbitals, as shown in Figure 1. A perpendicular plane reflects the same coefficients and signs of the wave function of each quinone unit.

Geometry optimization was also performed on the D−A system **10a** and **10b**, and the same conclusions were reached in terms of the localization of the HOMO and LUMO coefficients and energies (for **10a**, HOMO = −5.04 eV, LUMO = −3.67 eV; for **10b**, HOMO = −4.90 eV, LUMO= −3.69 eV) with an estimated gap of 1.37 eV for **10a** and 1.21 eV for **10b**.

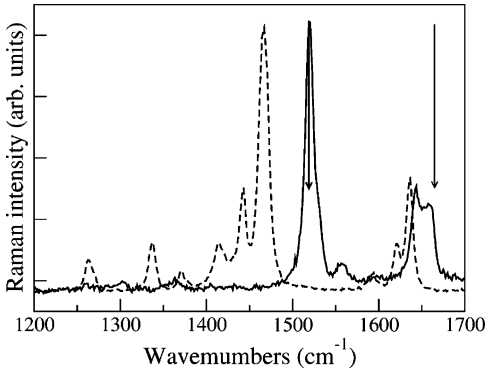


**FIGURE 2.** Raman spectra of **9** (continuous line) and **10a** (dashed line), 568 nm excitation. The arrows indicate the position of the C=O and C=C stretchings in the Raman spectra of neutral *p*-benzoquinone and TTF crystals, respectively.

All spectroscopic data ($^1H$ and $^{13}C$ NMR, MS, IR, Raman) were in agreement with the described structures of **9** and **10a**. Particularly, these compounds appeared to be especially stable. As suggested first by the presence of the molecular peak as the base peak in mass spectrometry, this stability was confirmed by the thermal gravimetric analysis (TGA) study, which showed the beginning of the decomposition at 240 and 290 °C for **9** and **10a**, respectively. The Raman spectrum of D−A **10a** (Figure 2) showed a clear downward shift of both carbonyl (∼1630 $cm^{-1}$) and central C=C (1446 $cm^{-1}$) stretching of the quinone and TTF units, respectively, with respect to the corresponding values (∼1665 and 1518 $cm^{-1}$) of neutral *p*-benzoquinone[24] and neutral TTF.[25] A less pronounced downward shift was observed for the C=O stretching of A−D−A **9**, whereas the TTF C=C stretching is practically unshifted in this case (Figure 2; the frequencies are at ∼1655[24] and 1522 $cm^{-1}$). The same trend was found in the IR spectra, where the carbonyl antisymmetric stretch is located at 1650 and at 1648 $cm^{-1}$ for **9** and **10a**, respectively, to be compared to about 1665 $cm^{-1}$ for *p*-benzoquinone.[24] This behavior indicated a partial charge transfer from the TTF core to the carbonyl groups of the quinone moiety. The charge transfer was rather small for **9** but increased in the asymmetric unit **10a** and, in the solid state, could have both intra- and intermolecular character (see below).

(22) Phosphonate **17** was synthesized according to well-established procedures from corresponding substituted 1,3-dithiole-2-thione: Moore, A. J.; Bryce, M. R. *Synthesis* **1991**, 26.

(23) Frisch, M. J.; Trucks, G. W.; Schlegel, H. B.; Scuseria, G. E.; Robb, M. A.; Cheeseman, J. R.; Zakrzewski, V. G.; Montgomery, J. A., Jr.; Stratmann, R. E.; Burant, J. C.; Dapprich, S.; Millam, J. M.; Daniels, A. D.; Kudin, K. N.; Strain, M. C.; Farkas, O.; Tomasi, J.; Barone, V.; Cossi, M.; Cammi, R.; Mennucci, B.; Pomelli, C.; Adamo, C.; Clifford, S.; Ochterski, J.; Petersson, G. A.; Ayala, P. Y.; Cui, Q.; Morokuma, K.; Malick, D. K.; Rabuck, A. D.; Raghavachari, K.; Foresman, J. B.; Cioslowski, J.; Ortiz, J. V.; Stefanov, B. B.; Liu, G.; Liashenko, A.; Piskorz, P.; Komaromi, I.; Gomperts, R.; Martin, R. L.; Fox, D. J.; Keith, T.; Al-Laham, M. A.; Peng, C. Y.; Nanayakkara, A.; Gonzalez, C.; Challacombe, M.; Gill, P. M. W.; Johnson, B. G.; Chen, W.; Wong, M. W.; Andres, J. L.; Head-Gordon, M.; Replogle, E. S.; Pople, J. A. *Gaussian 98*, revision A.9; Gaussian, Inc.: Pittsburgh, PA, 1998.

(24) Liu, R.; Zhou, X.; Pulay, P. *J. Phys. Chem.* **1993**, *96*, 4255 and references therein. Notice that in both Raman and IR, the carbonyl stretching bands are affected by Fermi resonance. We believe that the doublet structure seen in the Raman spectra of **9** and **10a** (Figure 2) share the same origin. Accordingly, in the text we report as an approximate frequency the corresponding average.

(25) Bozio, R.; Zanon, I.; Girlando, A.; Pecile, C. *J. Chem. Phys.* **1979**, *71*, 2282.

**SCHEME 2. Polarization of the S−C═C−C═O Conjugated System of Triad 9 Supported by the Charge Distribution Obtained by Theoretical Calculations and in Agreement with the Polarization Suggested for Compound 19[26]**

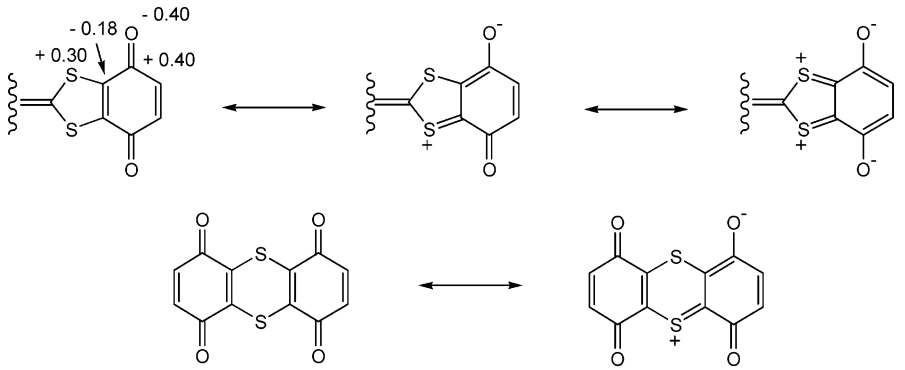


19

On the other hand, this influence of TTF on the benzoquinone moiety was shown in solution by comparing the $^{13}C$ spectra of **9** and **10a** with that of *p*-benzoquinone itself. Although the $^{13}C$ chemical shift of the carbonyl functionality appeared at 187.1 ppm ($CDCl_3$ as the reference) for *p*-benzoquinone, the upfield shift to 177.9 and 177.7 ppm for the corresponding carbon of **9** and **10a**, respectively, should result from the displacement of the electron density caused by the push−pull S−C═C−C═O system, suggesting the mesomeric form shown in Scheme 2. This resonance form was previously proposed for the bis(*p*-benzoquinone) **19**, which showed a maximum absorption at 508 nm in acetonitrile.[26] The charge distribution calculated by DFT methods on the neutral compound **9** was in complete agreement with a strong polarization of the S−C═C−C═O conjugated system and strongly supported the partial zwitterionic nature of the ground state (Scheme 2).

The electronic absorption spectrum of **9** confirmed the existence of the electronic interaction between both D and A moieties, and comparatively, the effect of the strong donor tetrathiafulvalene became evident. The UV−visible spectra of **9** showed the presence of a broad absorption band in the 500−1100 nm region, with the strongest absorption evidenced in $CS_2$ and centered at ca. 808 nm, which clearly indicates a weak charge-transfer interaction resulting from the conjugation involving both donor and acceptor moieties (Figure 3).

The measurement at different concentrations proved the intramolecular nature of this charge transfer from donor to acceptor moiety. A red-shift effect was observed for **10a**, which presented a broad absorption band between 600 and 1300 nm centered at ca. 892 nm in $CS_2$. For both **9** and **10a**, the position of the band just corresponds to the HOMO−LUMO gap calculated as described above. These D−A and A−D−A compounds exhibited strong solvatochromism of the charge-transfer band depending on the polarity of solvents (Table 1).

**Electrochemical Properties of Fused TTF−Quinone(s) 9 and 10a.** The cyclic voltammogram of D−A **10a** (*n*-$Bu_4NPF_6$ 0.1 M in $CH_2Cl_2$/acetonitrile 9/1) showed two one-electron reversible oxidation waves at $E_{ox1}^0 = +0.74$ V and $E_{ox2}^0 = +1.11$ V (vs Ag/AgCl) corresponding to the successive generation of the cation radical and dication of the TTF moiety. Two reduction processes were shown for the *p*-benzoquinone moiety, including the first one-electron reversible reduction wave at $E_{red1}^0 = -0.21$ V (Figure 4) and the second reduction wave $E^0_{red2}$ at approximately −1.20 V, which was not reversible in these experimental conditions. Concerning the A−D−A compound **9**, the oxidation potentials were clearly shifted to more positive values ($E_{ox1}^0 = +0.99$ and $E_{ox2}^0 = +1.36$ V, vs Ag/AgCl), the electron-withdrawing effect of the quinone group being responsible for this phenomenon. The *p*-benzoquinone moiety was characterized by a two-electron reversible reduction wave $E_{red1}^0$ approximately at −0.25 V. In fact, a splitting of this first reduction wave ($E_{red1}^0 = -0.20$ V and $E_{red1'}^0 = -0.28$ V) was observed by

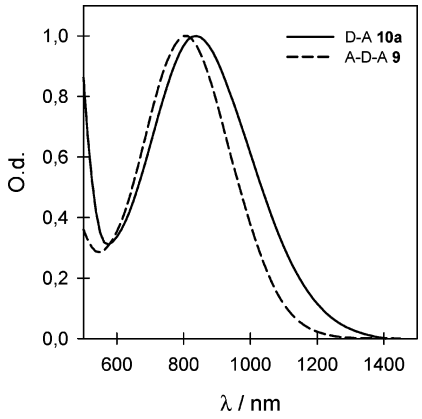


**FIGURE 3.** Electronic absorption spectra of **9** and **10a** in $CS_2$.

**TABLE 1. Wavelength of the Charge Transfer UV−vis Absorption Maxima of A−D−A 9 and D−A 10a in Solvents of Varying Polarity[a]**

| solvent | A−D−A **9** ($\lambda$ nm) | D−A **10a** ($\lambda$ nm) |
|---|---|---|
| DMSO | 670 | 762 |
| DMF | 735 | 758 |
| acetonitrile | 738 | 776 |
| toluene | 773 | 820 |
| dichloromethane | 782 | 847 |
| $CCl_4$ | 804 | 863 |
| $CS_2$ | 808 | 892 |

[a] Extinction molar coefficient of this charge transfer band was determined for **9** and **10a** in toluene to be 780 and 425 $M^{-1}$ $cm^{-1}$, respectively.

(26) Hünig, S.; Siunzger, K.; Bau, R.; Metzenthin, T.; Salbeck, J. *Chem. Ber.* **1993**, *126*, 465.

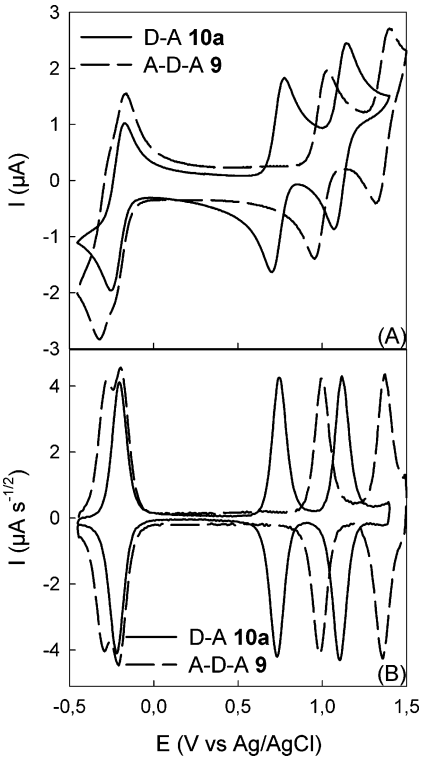


**FIGURE 4.** Cyclic voltammograms (top) and their corresponding deconvolution (bottom) of D−A **10a** and triad **9**; Pt electrode vs Ag/AgCl, $n$Bu$_4$NPF$_6$ 0.1 M in $CH_2Cl_2/CH_3CN$ 9/1, $10^{-3}$ M, $v$ = 500 mV/s. The second reduction waves are not presented on this figure.

using a slowest scan rate or cyclic voltammogram deconvolution. Thus, the successive generation of Q−TTF−Q$^{-\bullet}$ and Q$^{-\bullet}$−TTF−Q$^{-\bullet}$ species was observed. This phenomenon of splitting showed that the electrochemical behavior of both *p*-benzoquinone moieties is resulting from modifications on the electronic interaction between TTF and *p*-benzoquinone moieties at the Q−TTF−Q$^{-\bullet}$ stage and from Coulombic repulsion between reduced species at the Q$^{-\bullet}$−TTF−Q$^{-\bullet}$ stage. The values corresponding to the difference between the oxidation potential and the electron affinity were experimentally determined to be 1.19 eV for triad A−D−A **9** and 0.95 eV for dyad D−A **10a**, by calculating the difference between the first oxidation peak of TTF ($Ep_a$) and the first reduction peak of *p*-benzoquinone ($Ep_c$).

To clearly observe the second two-electron reduction waves of the *p*-benzoquinone moiety, we performed experiments using *o*-dichlorobenzene/acetonitrile (19/1) as the mixture of solvents. The cyclic voltammogram of triad **9** exhibited two reversible one-electron oxidation processes with redox potentials $E_{ox1}{}^0$ and $E_{ox2}{}^0$ at +0.97 and +1.34 V (vs Ag/AgCl), respectively, and two independent reduction processes. After deconvolution, the first reversible system was shown as two successive reductive steps corresponding to the generation of Q−TTF−Q$^{-\bullet}$ and Q$^{-\bullet}$−TTF−Q$^{-\bullet}$ species with redox potentials $E_{red1}{}^0$ and $E_{red1'}{}^0$ at −0.33 and −0.40 V, respectively. The second quasi-reversible system showed one broad wave corresponding to the reduction into Q$^{2-}$−TTF−Q$^{-\bullet}$ and Q$^{2-}$−TTF−Q$^{2-}$ species at −1.16 V (Figure 5).

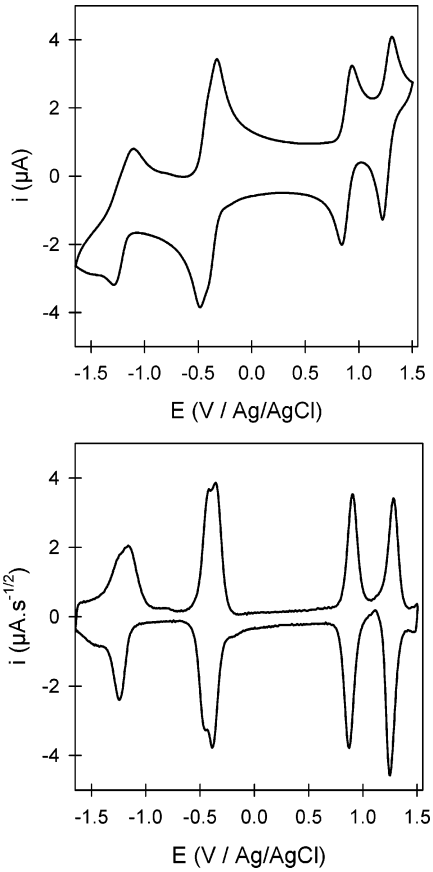


**FIGURE 5.** Cyclic voltammogram (top) and its deconvolution (bottom) of triad **9**; Pt electrode vs Ag/AgCl, $n$Bu$_4$NPF$_6$ 0.1 M in *o*-dichlorobenzene/$CH_3CN$ 19/1, 5 × $10^{-4}$ M, $v$ = 200 mV/s.

As the bis(1,4-benzoquinone)TTF **9** was clearly characterized in terms of cyclic voltammetry, we were interested in the problem resulting from the bis(1,4-naphthoquinone)TTF **8** and the absence of electroactive species of this compound upon oxidation as noted by W. H. Watson et al.[16] We therefore applied our synthetic methodology to synthesize the bis(1,4-naphthoquinone)-TTF (Scheme 3). Thus, the reaction of 2,3-dichloronaphthoquinone with potassium sulfide and carbon disulfide in DMF, followed by treatment with sodium dithionite, afforded the 2-thioxo-1,3-dithiole derivative **20** as described.[16] Precursor **22** was obtained by acetylation using acetic anhydride in the presence of triethylamine in 79% yield and transchalcogenation by treatment with mercuric acetate in glacial acetic acid in 96% yield. Triethyl phosphite coupling reaction was performed, affording the tetrathiafulvalene derivative **23** in 53% yield. The conversion into quinone functionality described herein was successfully carried out using DDQ, affording in 68% yield the bis(1,4-naphthoquinone)TTF **8** as a light green powder, this characteristic being in agreement with the compound previously reported.[16]

Despite its very low solubility, this compound **8** was studied by cyclic voltammetry using $n$-Bu$_4$NPF$_6$ 0.1 M as a supporting electrolyte and *o*-dichlorobenzene/acetonitrile (19/1) as the mixture of solvents (2 × $10^{-4}$ M, $v$ = 200 mV/s). In contradiction with previous observation,[16] compound **8** was characterized by two reversible oxidation and two reduction waves attributed to the TTF and naphthoquinone moieties, respectively, this cyclic voltam-

**SCHEME 3**[a]

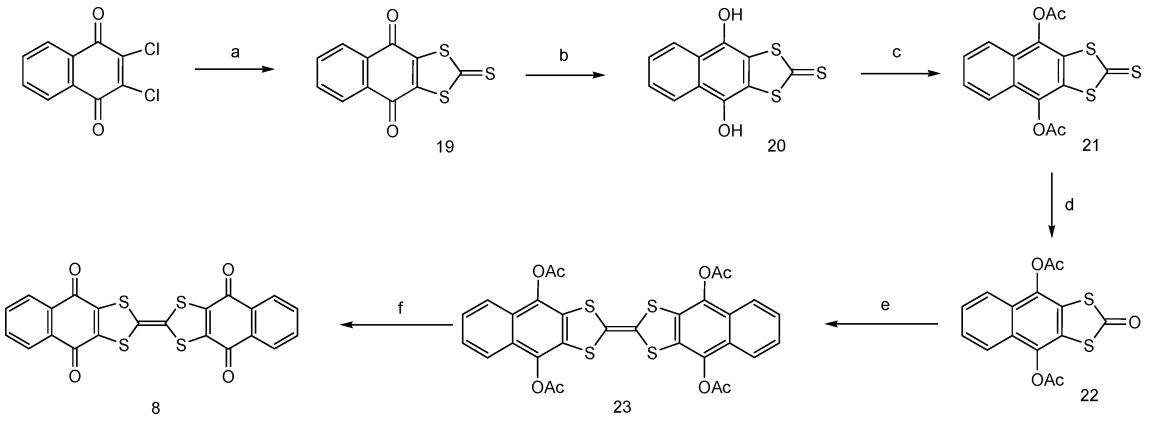


[a] Reagents: (a) $K_2S$, $CS_2$, DMF, 65% (lit.[16a] 63%). (b) $Na_2S_2O_4$, 75% (lit.[16a] 97%). (c) $Ac_2O$, $Et_3N$, 79%. (d) $Hg(OAc)_2$, $CH_2Cl_2$/glacial AcOH, 96%. (e) Δ $P(OEt)_3$, 53%. (f) (i) MeONa/MeOH; (ii) PTSA, $H_2O$; (iii) DDQ, 68%

mogram being similar to that obtained for **9** (Figure 5). Thus, the two oxidation waves corresponding to the formation of the cation radical and dication of the TTF were shown at +0.96 and +1.35 V (vs Ag/AgCl), respectively. The first reduction process appeared as a split system with two different waves at −0.56 and −0.61 V and the second reduction process as a broad wave at −1.20 V.

**Properties of Oxidized and Reduced Species from Triad 9 and Dyad 10a.** The optical properties of the cation radical and dication of bis(1,4-benzoquinone)-TTF **9** were investigated by in situ UV−vis−NIR spectroscopy, by addition of increasing amounts of $NOBF_4$. Chemical oxidation led to the rapid disappearance of bands attributed to the neutral TTF derivative (broad band from 600 to 1100 nm centered at 782 nm) and to the development of new bands characteristic for the cation radical (434, 580 nm) and the dication (566 nm) (Figure 6).[27] The values of the HOMO−LUMO difference calculated by DFT methods followed the same trend as the UV−visible data and were estimated to be 1.50 eV for $\mathbf{9}^{+\bullet}$ (HOMO = −9.65 eV, LUMO = −8.15 eV) and 1.82 eV for $\mathbf{9}^{2+}$ (HOMO = −14.46 eV, LUMO = −12.54 eV). As for the neutral molecule **9**, the optimized geometry found for the cation radical $\mathbf{9}^{+\bullet}$ was almost planar, while the dication $\mathbf{9}^{2+}$ presented distortion from planarity of 14°.[28] This torsion angle in the geometry of $\mathbf{9}^{2+}$ may be related to increasing *σ*-character in the C−C central bond between the two 1,3-dithiolium moieties. This is supported by the optimized central bond lengths, computed as 1.35 Å for the neutral molecule **9**, 1.40 Å for the cation radical $\mathbf{9}^{+\bullet}$, and 1.44 Å for the dication $\mathbf{9}^{2+}$.

The cation radical $\mathbf{9}^{+\bullet}\cdot\mathbf{CF_3SO_3}^-$ was also chemically prepared as a pure solid by oxidation of the triad **9** by using as an oxidizing agent iodobenzene diacetate in the presence of triflic acid according to a synthetic approach recently reported for the efficient stoichiometric control of TTF-derived cation radicals.[29] The IR spectrum of $\mathbf{9}^{+\bullet}\cdot\mathbf{CF_3SO_3}^-$ clearly showed the appearance of strong bands at 1255, 1027, and 636 $cm^{-1}$ characteristic of the $SO_3^-$ anion.[29] The most evident change in the Raman spectrum is the downward shift of the TTF central double-band stretch from 1519 to 1399 $cm^{-1}$. The ESR signal of an acetone solution of the cation radical salt $\mathbf{9}^{+\bullet}\cdot\mathbf{CF_3SO_3}^-$ exhibited the expected quintet ($g$ = 2.0071), showing a small coupling of the electronic spin with the four equivalent hydrogen atoms of the quinone moieties ($a_H$ = 0.36 G). Moreover, the $^{33}S$ hyperfine coupling constant was also observed upon amplification of the spectrum ($a_S$ = 4.1 G).

The anion radical $\mathbf{9}^{-\bullet}\cdot\mathbf{P(C_6H_5)_4}^+$, as well as a pure solid, was prepared by chemical reduction with Cu metal in $CH_2Cl_2$ containing tetraphenylphosphonium bromide. This compound is highly insoluble, and a very fine precipitate is formed almost at the beginning of the

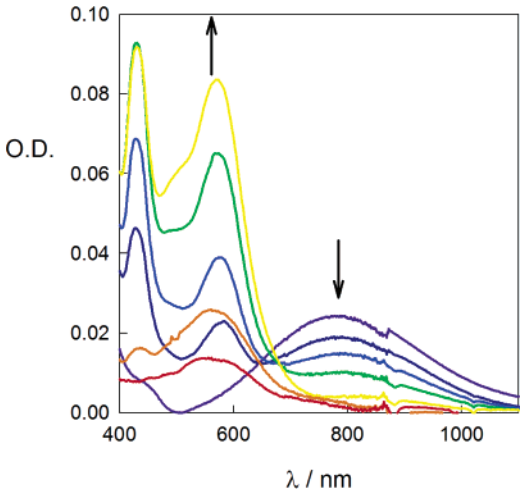


**FIGURE 6.** Evolution of the optical spectrum for the neutral triad **9** ($3 \times 10^{-4}$ M in $CH_2Cl_2$) upon oxidation using $NOBF_4$ in $CH_3CN$ solution.

(27) For references on calculated and experimental UV−visible absorption of cation radical and dication of TTF derivatives, see: (a) Khodorkovsky, V.; Shapiro, L.; Krief, P.; Shames, A.; Mabon, G.; Gorgues, A.; Giffard, M. *Chem. Commun.* **2001**, 2736. (b) Andreu, R.; Garín, J.; Orduna, J. *Tetrahedron* **2001**, *57*, 7883.

(28) This distortion from planarity between the two dithiolium rings was previously observed on the crystal structure of the dication from the unsymmetrical outer S-position isomer of BEDT-TTF. Hudhomme, P.; Le Moustarder, S.; Durand, C.; Gallego-Planas, N.; Mercier, N.; Blanchard, P.; Levillain, E.; Allain, M.; Gorgues, A.; Riou, A. *Chem. Eur. J.* **2001**, *7*, 5070.

(29) Giffard, M.; Mabon, G.; Leclair, E.; Mercier, N.; Allain, M.; Gorgues, A.; Molinié, P.; Neilands, O.; Krief, P.; Khodorkovsky, V. *J. Am. Chem. Soc.* **2001**, *123*, 3852.

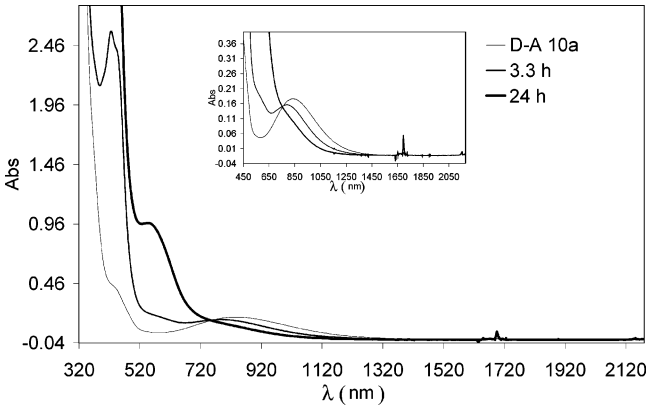


**FIGURE 7.** Evolution of the UV−vis−NIR spectrum during the course of the reduction of D−A **10a**, at different times of reaction. The inset is the enlargement of the vis−NIR part.

reduction process. The IR spectrum of $\mathbf{9}^{-\bullet}\cdot\mathbf{P(C_6H_5)_4}^{+}$ showed important modifications on the band corresponding to carbonyl groups and the appearance of characteristic P−C bands at 650−750 $cm^{-1}$. Isolated pure solid $\mathbf{9}^{-\bullet}\cdot\mathbf{P(C_6H_5)_4}^{+}$ is insoluble in most of the common organic solvents. A much diluted solution can only be prepared in ethyl acetate and presents a very weak ESR signal consisting of five lines. The high degree of insolubility of $\mathbf{9}^{-\bullet}\cdot\mathbf{P(C_6H_5)_4}^{+}$ prevents the quantitative study of the UV−vis−NIR spectra of the compound as well as the generation of the dianionic derivative $\mathbf{9}^{2-}$. An ESR study of the anion radical species $\mathbf{9}^{-\bullet}\cdot\mathbf{P(C_6H_5)_4}^{+}$ generated "in situ" is presented below.

DFT calculations were performed for a full geometry optimization of the anion radical Q−TTF−$Q^{-\bullet}$ system. The optimized geometry found for the anion radical $\mathbf{9}^{-\bullet}$ was perfectly planar. The calculation performed was unrestricted, and then each orbital obtained was a spin−orbital with single occupancy. The molecular orbital analysis showed that the HOMO orbital (singly occupied spin−orbital), with a calculated energy of −1.40 eV, presented the same shape (and coefficients) as the LUMO orbital of the neutral triad Q−TTF−Q **9**. The calculated energy value for the corresponding LUMO of the anion radical was −1.02 eV. We observed that the overall character for the single occupied HOMO and the corresponding LUMO was very similar to the LUMO of the neutral molecule: the only contributions on the HOMO and LUMO were located on the outer quinone part of the molecule.

Chemical reduction of the dyad **10a** with Cu metal in $CH_2Cl_2$ containing tetraphenylphosphonium bromide led to a decrease in the characteristic charge-transfer broad band of the neutral derivative and to the appearance and increase with reaction time of the bands due to the anion radical (425 and 550 nm)[30] (Figure 7). The ESR spectrum of this solution consists of a well-defined triplet ($g$ = 2.0046) arising from the coupling of the unpaired electron with the two equivalent hydrogen atoms of the quinone ($a_H$ = 2.50 G).

The presence on the same molecule of electron donor and acceptor(s) moieties allows the successive generation

(30) Zhao, X.; Imahori, H.; Zhan, C.-G.; Sakata, Y.; Iwata, S.; Kitagawa, T. *J. Phys. Chem.* **1997**, *101*, 622.

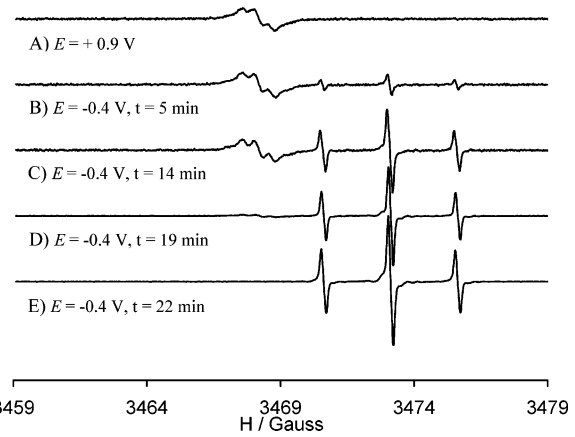


**FIGURE 8.** Evolution of the ESR spectra of dyad **10a** upon in situ electrooxidation (A) and subsequent electroreduction (B−E) (see text).

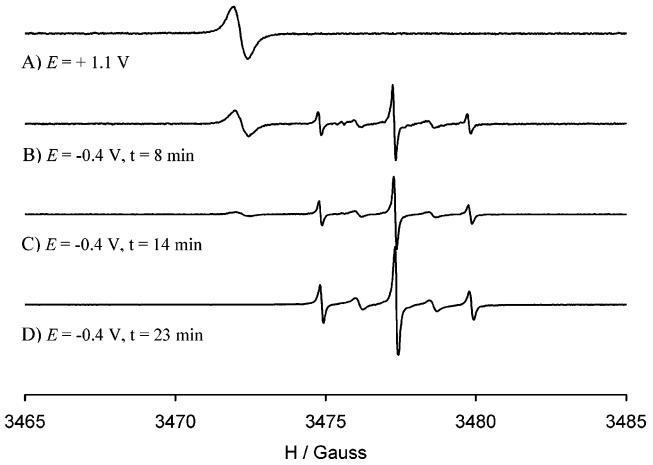


**FIGURE 9.** Evolution of the ESR spectra of triad **9** upon in situ electrooxidation (A) and subsequent electroreduction (B−D) (see text).

of their cation radical and anion radical derivatives upon oxidation or reduction, respectively. Thus, the cation radical $\mathbf{10a}^{+\bullet}$ was generated by electrochemical oxidation performed in an electrochemical cell adapted to the ESR spectrometer at +0.9 V (vs Ag/AgCl) in $CH_2Cl_2$ using $n$-$Bu_4NPF_6$ as an electrolyte and monitored by ESR spectroscopy (Figure 8).

The corresponding spectrum consisted of an overlapped triplet with the typical pattern of a coupling with the two equivalent quinonic protons ($g$ = 2.0075, $a_H$ = 0.46 G). By imposing a reduction potential at −0.40 V (vs Ag/AgCl), we could observe the slow disappearance of the signal corresponding to the cation radical and the appearance of the signal due to the anion radical $\mathbf{10a}^{-\bullet}$. The corresponding signal was the same as the species obtained by chemical reduction, which is a well-resolved triplet ($g$ = 2.0047, $a_H$ = 2.51 G). Using the same experimental procedure for triad **9** (Figure 9), we observed that the ESR spectrum for the cation radical $\mathbf{9}^{+\bullet}$ consisted of a poorly resolved quintet ($g$ = 2.0074) and, for the anion radical $\mathbf{9}^{-\bullet}$, of a quintet having the second and fourth lines considerably broader than the other three. The ESR signal of the anion radical was very

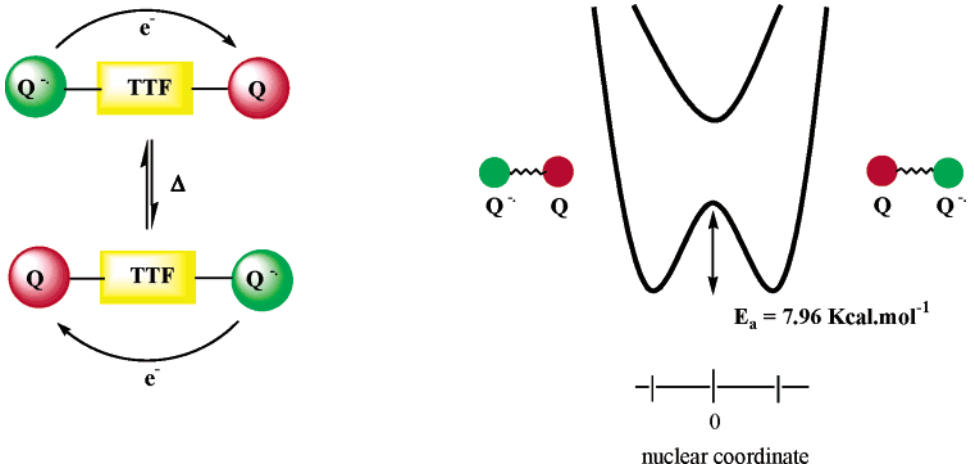


**FIGURE 10.** Intramolecular electron transfer proccess using the TTF as a bridge in the purely class II mixed-valence Q−TTF−Q$^{-\bullet}$ system.

**SCHEME 4. Electron Exchange through the TTF Bridge between the Two Quinonic Centers**

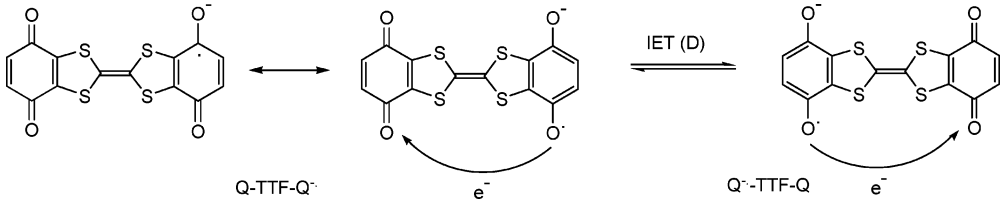


similar (although much more intense) to the one obtained from the ethyl acetate solution of solid **9**$^{-\bullet}$·**P(C$_6$H$_5$)$_4$**$^+$.

The specific features observed in the ESR spectrum for the anion radical **9**$^{-\bullet}$ can be considered as the signature of a dynamic process observed in the ESR time scale.[31] Taking into account that the cyclic voltammogram of the Q−TTF−Q triad **9** suggested an effective electronic coupling between both quinone centers by the presence of two distinguishable reduction processes ($\Delta E$ = 80 mV), the dynamic process can be attributed to the electron transfer between both quinones. To characterize this process, we performed the temperature dependence study of the ESR spectra of the mixed-valence species **9**$^{-\bullet}$. For comparison purposes, the anion radical of dyad **10a** was also investigated in the same way. Both species were generated by chemical reduction with Cu metal in different solvents containing tetraphenylphosphonium bromide.

The characteristic ESR spectrum of the anion radical TTF−Q$^{-\bullet}$ **10a**$^{-\bullet}$ that consists of three lines with 1:2:1 intensities was singularly invariant over a wide temperature range between 270 and 325 K in $CH_2Cl_2$ and between 260 and 340 K in a 10:1 mixture of ethyl acetate/*tert*-butyl alcohol. On the contrary, the ESR spectrum of the anion radical Q−TTF−Q$^{-\bullet}$, prepared under the same conditions, changed upon cooling from 340 to 260 K.[32] Thus, whereas the spectrum at 260 K was essentially identical with that of the analogue TTF−Q$^{-\bullet}$ (three 1:2:1 lines, $a_H$ = 2.47 G (2H)), at higher temperatures (from 330 to 340 K), the spectra were characterized by couplings with two more equivalent protons (five lines 1:4:6:4:1, $a_H$ = 1.23 G (4H)).[33] As the temperature was gradually decreased from 340 to 260 K, alternant lines broadened due to the dynamic electron exchange between both quinone electrophores through the TTF bridge (Scheme 4).[34] The low-temperature spectra of Q−TTF−Q$^{-\bullet}$ unequivocally demonstrated that the odd electron was localized on one quinone unit at the ESR time scale and the activation energy barrier was overcome by thermal stimulus to promote an intramolecular electron transfer (IET) process.[17] It is important to indicate that this IET process can only be studied in all its extension using a 10:1 mixture of ethyl acetate/*tert*-butyl alcohol. Due to the high insolubility of the Q−TTF−Q$^{-\bullet}$ mixed-valence species, it was not possible to perform a quantitative study of the IET process by vis−NIR spectroscopy.

We have clearly demonstrated for the first time that TTF can be used as a bridge promoting electron conduction between two redox centers and that the triad **9** is therefore the prototype of mixed-valence compound able to undergo fast intramolecular electron transfer through this bridge (Figure 10).[35]

With the aim of developing devices using the direct electronic conduction through single molecules,[36] our interest was then focused on the study of the role of various parameters governing the IET rates. The dynam-

(31) Weil, J. A.; Bolton, J. R.; Wertz, J. E. *Electron Paramagnetic Resonance*; John Wiley & Sons: New York, 1994.

(32) Spectra were recorded at the very beginning of the reduction process. At this stage, the major species present in the solution is the ESR silent neutral compound **9**. The observed ESR signal is due to the anion radical, since for statistical reasons dianion radical must have a negligible concentration.

(33) As the coupling constant $a_H$ is dependent on the spin density, the delocalization of the electron over both quinones requires that this coupling constant is two times less for compound **9** than for **10a**: $a_H = (8\pi g_e/3g_o)\gamma_H\beta_H\rho_H(r_H)$. $g_e/g_o$ is the ratio of the isotropic $g$ value for the radical to that of the free electron; $\gamma_H$ and $\beta_H$ are the gyromagnetic nuclear ratio and the nuclear magneton, respectively, and $\rho_S(r_H)$ is the spin density on the nucleus of the hydrogen atom.

(34) Hudson, A.; Luckhurst, G. R. *Chem. Rev.* **1969**, *69*, 1961.

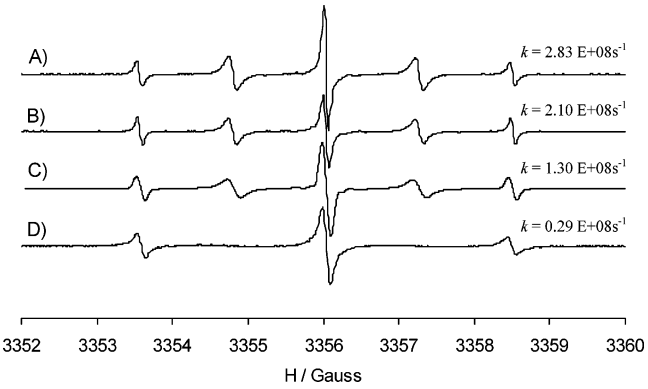


**FIGURE 11.** ESR spectra of Q−TTF−Q$^{-\bullet}$P$(C_6H_5)_4^+$ at 300 K, generated "in situ" in different solvents. (A) Dichloromethane, (B) ethyl acetate, (C) ethyl acetate/ *tert*-butyl alcohol 10:1, and (D) *tert*-butyl alcohol.

ics of the intramolecular exchange process was simulated using the Heinzer program,[37] and first-order rate constants were extracted by fitting the experimental spectra. The values obtained by simulation of all spectra obtained in a 10:1 mixture of ethyl acetate/*tert*-butyl alcohol led to a linear Arrhenius plot over the range 340−260 K, giving the following activation parameters: $E_{act} = 7.96$ kcal/mol; log $A = 13.9$ ($\Delta G^{\ddagger}_{298K} = 6.4$ kcal/mol, $\Delta H^{\ddagger} = 7.4$ kcal/mol, and $\Delta S^{\ddagger} = 3.1$ eu). As expected, the rate constant of the IET process varied with the solvent used due to the energy variation resulting from solvent reorganization.[32] In Figure 11, the differences in the rate constant at 300 K in dichloromethane, ethyl acetate, *tert*-butyl alcohol, and a 10:1 mixture of ethyl acetate/*tert*-butyl alcohol were clearly observed by the variation of the ESR spectra.

The Q−TTF−Q$^{-\bullet}$ species is therefore a prototypical class II mixed-valence system[38] involving moderately coupled redox centers as indicated by cyclic voltammetry results. This system can be compared with polyacene diquinones **24**−**26** as fused weak donors and acceptors previously reported (Scheme 5). It was also demonstrated that the odd electron of the anion radical of **24** was delocalized,[39] and on the contrary, the anion radicals derived from **25** and **26** were not delocalized and could then formally be considered as mixed-valence species.[40] Indeed, the optical spectra suggested that the unpaired electron on these anion radicals were localized on each subunit and was hopping from one side to another. Such an interpretation was confirmed by temperature-variable ESR spectra, and it would be interesting to note that the activation parameters previously reported for the anion radical of anthracene-diquinone **26**[41] were close to those determined for the anion radical Q−TTF−Q$^{-\bullet}$.

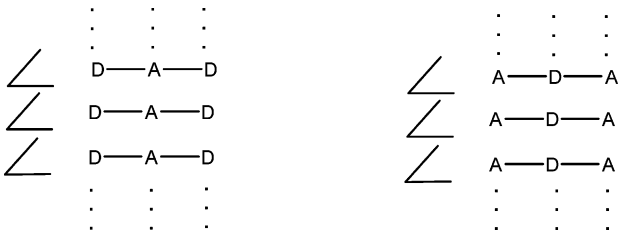


**FIGURE 12.** Segregated stacks of D−A−D or A−D−A systems.

**SCHEME 5. Crystallographic and Single-Crystal IR Studies**

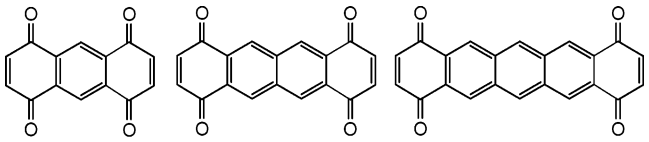


**Crystallographic and Single-Crystal IR Studies.** The packing mode in the crystals of these materials is a crucial parameter of their potential ability to reach conductivity.[18] To obtain such conducting-linked donor−acceptor complexes, the most important architectural requirement was the aggregation in the solid state of both donors (D) and acceptors (A) in segregated stacks, as extended in the approach of D−A−D[42] and A−D−A[43] systems for which the tendency to produce the corresponding stacking motifs was observed (Figure 12).

Although the weak donor and acceptor character of both moieties usually implies mixed stacks, diquinone derivatives can serve as an example of the A−D−A motif characterized by segregated stacking, showing an almost ideal one-dimensional array of quinone and phenyl

(35) Other organic systems presenting IET between redox centers have been previously reported: (a) Nelsen, F. S.; Thomson-Colon, J. A.; Katfory, M. *J. Am. Chem. Soc.* **1994**, *116*, 1589. (b) Bonvoisin, J.; Launay, J.-P.; Rovira, C.; Veciana, J. *Angew. Chem., Int. Ed. Engl.* **1994**, *33*, 2106. (c) Lahlil, K.; Moradpour, A.; Bowlas, C.; Menou, F.; Cassoux, P.; Bonvoisin, J.; Launay, J.-P.; Dive, G.; Dehareng, D. *J. Am. Chem. Soc.* **1995**, *117*, 9995. (d) Nelsen, F. S.; Ismagilov, R. F.; Trieber, D. A. *Science* **1997**, *278*, 846. (e) Lambert, C.; Nöll, G. *Angew. Chem., Int. Ed.* **1998**, *37*, 2107. (f) Lambert, C.; Nöll, G. *J. Am. Chem. Soc.* **1999**, *121*, 8434. (g) Ruiz-Molina, D.; Sedó, J.; Rovira, C.; Veciana, J. In *Handbook of Advanced Electronic and Photonic Materials and Devices*; Nalwa, H. S., Ed.: Academic Press: San Diego, 2001; Vol. 3, p 303. (h) Launay, J. P. *Chem. Soc. Rev.* **2001**, *30*, 386. (i) Rovira, C.; Ruiz-Molina, D.; Elsner, O.; Vidal-Gancedo, J.; Bonvoisin, J.; Launay, J.-P.; Veciana, J. *Chem.—Eur. J.* **2001**, *7*, 240. (j) Mayor, M.; Büschel, M.; Fromm, K. M.; Lehn, J.-M.; Daub, J. *Chem. Eur. J.* **2001**, *7*, 1266. (k) Lambert, C.; Nöll, G.; Schelter, J. *Nat. Mater.* **2002**, *1*, 69. (l) Lindeman, S. V.; Rosokha, S. V.; Sun, D.; Kochi, J. K. *J. Am. Chem. Soc.* **2002**, *124*, 842.

(36) (a) Bumm, L. A.; Arnold, J.; Cygan, M. T.; Dunbar, T. D.; Burgin, T. P.; Jones, L. II; Allara, D. L.; Tour, J. M.; Weiss, P. S. *Science* **1996** *271*, 1705. (b) Reed, M. A.; Zhou, C.; Muller, C. J.; Burgin, T. P.; Tour, J. M. *Science* **1997**, *278*, 252. (c) Metzger, R. M. *Acc. Chem. Res.* **1999**, *32*, 950. (d) Collier, C. P. Wong, E. W.; Belohradsky, M.; Raymo, F. M.; Stoddart, J. F.; Kuekes, P. J.; Williams, R. S.; Heath, J. R. *Science* **1999**, *285*, 391. (e) Joachim, C.; Gimzewski, J. K.; Aviram, A. *Nature* **2000**, *408*, 541. (f) Tour, J. M. *Acc. Chem. Res.* **2000**, *33*, 791. (g) Batchtold, A.; Hadley, P.; Nakanishi, T.; Dekker, C. *Science* **2001**, *294*, 1317. (h) Scandola, F., Chiorboli, C., Indelli, M. T., Rampi, M. A., Eds.; *Electron Transfer in Chemistry*; Wiley-VCH: New York, 2001; Vol. 3.

(37) Heinzer, J. *Mol. Phys.* **1971**, *22*, 167; *Quantum Chemistry Program Exchange* **1972**, No. 209. We thank Prof. A. Lund for a copy of this program.

(38) Robin, M. B.; Day, P. *Adv. Inorg. Chem. Radiochem.* **1967**, *10*, 247. Mixed-valence compounds are classified in three categories: (a) the redox centers are completely localized and behave as separated entities (class I), (b) intermediate coupling between the mixed-valence centers exists (class II), or (c) the system is completely delocalized and the intermediate redox states are attributed to the redox centers (class III).

(39) Jozefiak, T. H.; Miller L. L. *J. Am. Chem. Soc.* **1987**, *109*, 6560.

(40) Jozefiak, T. H.; Almlöf, J. E.; Feyereisen, M. W.; Miller, L. L. *J. Am. Chem. Soc.* **1989**, *111*, 4105.

(41) Rak, S. F.; Miller, L. L. *J. Am. Chem. Soc.* **1992**, *114*, 1388.

(42) Becker, J. Y.; Bernstein, J.; Bittner, S.; Levi, N.; Shaik, S. S.; Zer-Zion, N. *J. Org. Chem.* **1988**, *53*, 1689 and references therein.

(43) Le Paillard, M. P.; Robert, A.; Garrigou-Lagrange, C.; Delhaes, P.; Le Maguerès, P.; Ouahab, L.; Toupet, L. *Synth. Met.* **1993**, *58*, 233.

**SCHEME 6**

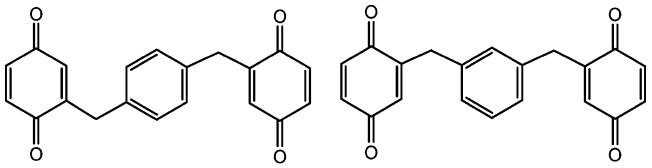

27 28

**TABLE 2. Bond Lengths and Intramolecular Interactions in the Triad 9 Determined by the X-ray Crystallographic Structure and DFT Calculations**

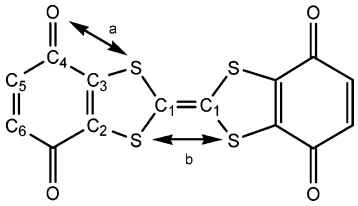

| | *a* | *b* | $C_1-C_1$ | $C_1-S$ | $S-C_3$ |
|---|---|---|---|---|---|
| crystallographic distance (Å) | 3.01(2) | 3.22(3) | 1.340(9) | 1.769(4) | 1.739(5) |
| calculated distance (Å) | 3.030 | 3.277 | 1.349 | 1.792 | 1.751 |

| | $C_3-C_2$ | $C_3-C_4$ | $C_4-O$ | $C_4-C_5$ | $C_5-C_6$ |
|---|---|---|---|---|---|
| crystallographic distance (Å) | 1.349(6) | 1.471(6) | 1.227(6) | 1.462(7) | 1.342(7) |
| calculated distance (Å) | 1.356 | 1.480 | 1.224 | 1.489 | 1.342 |

moieties for **27** and two-dimensional stacking for **28** (Scheme 6).[44]

Fine blue needles were obtained by slow evaporation of a solution containing the fused A−D−A system **9** in $CH_2Cl_2$/petroleum ether as a mixture of solvents. The X-ray crystallographic analysis revealed that the molecule is nearly planar, and only the carbonyl groups protruded from the molecular plane by 4°. This could be compared with the repulsion of the sulfur and oxygen lone pairs suggested in the case of **19**, for which the crystal structure showed that the carbonyl group protruded from the molecule plane by 2−10°.[26] Intramolecular S...O interactions were also shown [3.01(2) Å] between the oxygen atom of the quinone and the sulfur atom of TTF, this distance being shorter than the sum of the van der Waals radii of both atoms ($d$ = 3.25 Å).[45] Moreover, calculated bond lengths and intramolecular interactions were in good agreement with the corresponding distances determined from the crystallographic structure (Table 2).[46]

The packing arrangement of A−D−A molecules, involving a strong donor (TTF) and a weak acceptor (benzoquinone), was characterized by regular stacks along the *a* axis (Figure 13), as encountered in the vast majority of weak charge transfer complexes.

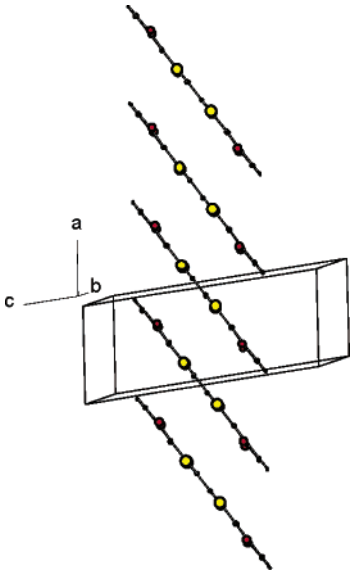


**FIGURE 13.** Regular stacking mode of TTF−diquinone molecules in the structure of **9**·$CH_2Cl_2$.

In fact, two consecutive molecules in stacks were shifted one from each other along the main molecular axis leading to a bond over cycle-type overlap between the central C=C bond of the TTF core and the benzene cycle of the acceptor (Figure 14a). Moreover, the bis(1,4-benzoquinone)TTF intermolecular distance between the face-to-face planes of the donor and acceptor moieties ($d$ = 3.60 Å) showed a significant overlap and may be compared to the plane-to-plane distances between donor and acceptor molecules in crystal packings of mixed-stack intermolecular charge transfer complexes.[47] For example, the interplanar distance between donor and acceptor molecules in the charge-transfer complex octamethylene-TTF−TCNQ is 3.53 Å. However, compared to the D...A interactions, compound **9** did not exhibit the infinite mixed stacking ...A..D..A..D.. motif: as a consequence of the shift mode of molecules, only [A...D...A]-type "triplets" were encountered in stacks along the direction perpendicular to the molecular plane (Figure 14b).

It must be noted that in the prototypical D−A−D system previously reported,[40,48] i.e., the dibenzylTCNQ compound involving a strong acceptor (TCNQ) and weak donors (benzyl), isolated triplets D...A...D formed by the central TCNQ ring of a molecule and two phenyl rings of two neighboring molecules were clearly observed. However, in this last structure, X-ray analysis also revealed a segregated mode of stacking for TCNQ parts,[17] which differed from the observed situation in **9** where TTF moieties did not form segregated stacks. The interstack CH(benzene cycle)...O(quinone) hydrogen bond interactions were of particular interest and seemed to strongly influence the crystal packing of triad **9**, leading to cyclic $R_2^2(8)$ motifs, according to Etter's representation,[49] and cavities in which disordered solvent molecules ($CH_2Cl_2$) were inserted (Figure 15).

(44) (a) Becker, J. Y.; Bernstein, J.; Bittner, S.; Shaik, S. S. *Pure Appl. Chem*. **1990**, *62*, 467. (b) Becker, J. Y.; Bernstein, J.; Bittner, S.; Giron, Y.; Harlev, E.; Kaufman-Orenstein, L.; Peleg, D.; Shahal, L.; Shaik, S. S. *Synth. Met*. **1991**, *41*−*42*, 2523.

(45) Bondi, A. *J. Phys. Chem*. **1964**, *68*, 441.

(46) Bond distances suggest a weak intramolecular charge transfer from TTF to benzoquinone moiety; see: Guionneau, P.; Kepert, C. J.; Bravic, D.; Chasseau, D.; Truter, M. R.; Kurmoo, M., Day, *P. Synth. Met*. **1997**, *86*, 1973.

(47) Chasseau, D.; Gaultier, J.; Fabre, J. M.; Giral, L. *Acta Crystallogr*. **1982**, *B38*, 1632.

(48) Becker, J. Y.; Bernstein, J.; Bittner, S.; Levi, N.; Shaik, S. S. *J. Am. Chem. Soc*. **1983**, *105*, 4468.

(49) Etter, M. C.; MacDonald, J. C. *Acta Crystallogr*. **1990**, *B46*, 256.

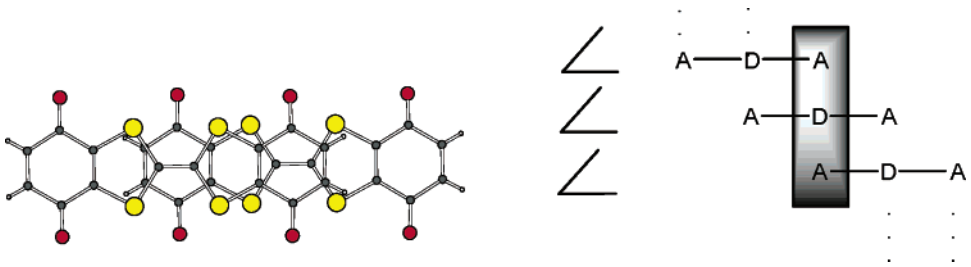


**FIGURE 14.** (left) Bond over cycle overlap type between two consecutive molecules in stacks and (right) schematic representation of the packing arrangement showing the A..D..A triplets.

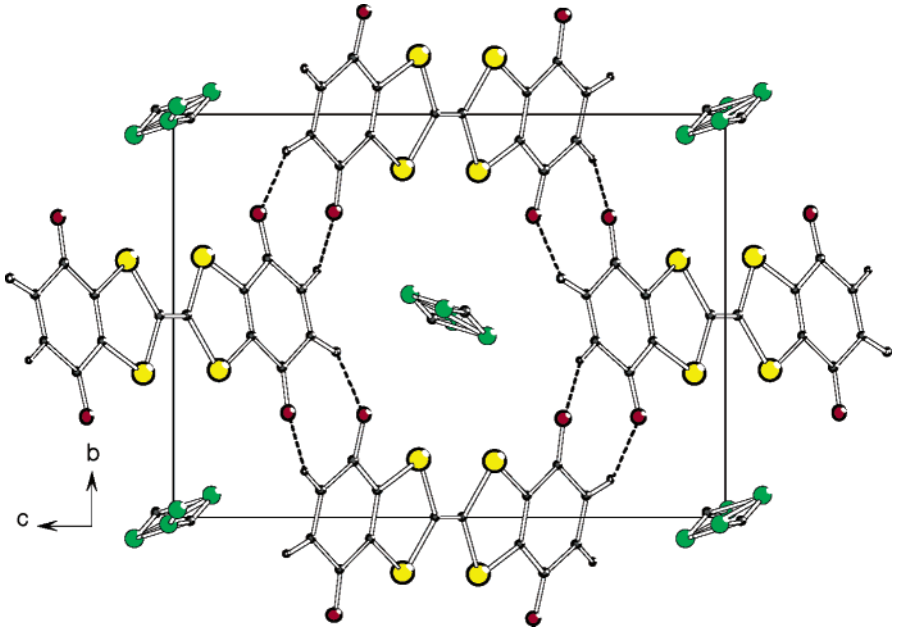


**FIGURE 15.** View of the crystal structure of **9**·$CH_2Cl_2$ along the stack axis showing intermolecular hydrogen bonding (dashed lines) and disordered $CH_2Cl_2$ molecules.

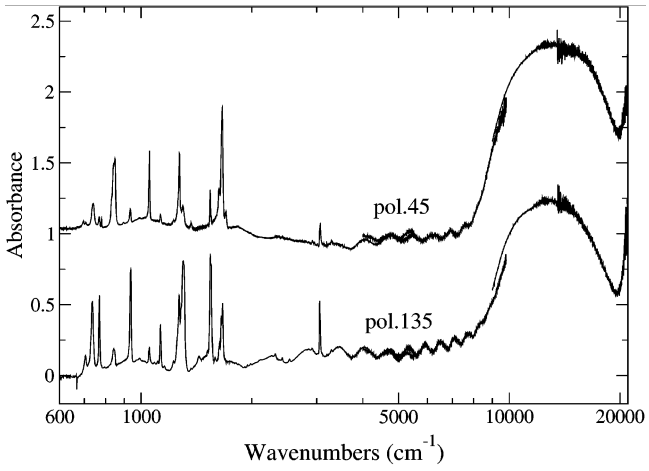


**FIGURE 16.** Polarized absorption spectra of A−D−A **9** from 600 to 21 000 $cm^{-1}$. Notice the logarithmic wavenumber scale. Beyond 4000 $cm^{-1}$, different beam splitters and polarizers have been used. No cosmetic changes have been made to reduce the noise or join the different spectral regions.

We have also obtained polarized IR and NIR−visible (from 600 to 21 000 $cm^{-1}$) absorption spectra of A−D−A crystal, as shown in Figure 16. The crystal plane was not identified, but it is likely *ac* (Figure 13). We have chosen the light polarizations to maximize the differences between the intensities of the IR bands. The electric vector of the radiation made an angle of approximately 45 and 135 degrees with respect to the needle axis. In addition to the IR features, the spectra displayed an electronic broad absorption centered around 13 000 $cm^{-1}$ (1.6 eV, 770 nm). The band was clearly associated with the intramolecular charge transfer transition identified above in the solution spectra. However, the band was not polarized, and a closer inspection of the spectra revealed a slightly different position of the band maxima in the two polarizations (the difference was about 500 $cm^{-1}$; notice the logarithmic scale in the wavenumber axis). Given the mixed stack motif of the crystal structure, we speculated that we observed *two* overlapping charge transfer transitions, one intra- and the other intermolecular. The two were orthogonal each other. If the above supposition was correct, A−D−A would represent a good example of a two-dimensional, "intra−inter" charge transfer crystal.

In any case, we have clearly shown that this fused and perfectly planar A−D−A assembly involving a strong donor (TTF) and a weak acceptor (quinone) had a high propensity to crystallize in the crystallographic arrangement characterized by the nonideal packing to reach conductivity, in contrast to nonfused A−D−A or D−A−D

systems **27** and **28**, respectively. In fact, the electrical conductivity measured on pellets using the four-probe technique was estimated to be $10^{-9}$ and $2 \times 10^{-9}$ S/cm for fused D−A **10** and A−D−A **9** systems, respectively, confirming the low degree of charge transfer in the undoped state.

## Conclusion

To control the stoichiometry between D and A, we have developed an interesting approach consisting of synthesizing TTF fused to acceptors such as *p*-benzoquinone. The quinone moiety of **9** and **10** can be used as a precursor for stronger acceptor moieties, e.g., DCNQI or TCNQ.[50] Consequently, work is in progress to improve this acceptor ability of the quinone moiety in order to reach unprecedented fused TTF−TCNQ (D−A) derivatives and TCNQ−TTF−TCNQ (A−D−A). Quinone- or TCNQ-based intramolecular donor−acceptor systems constitute a promising field of applications due to the interesting optoelectronic properties they can exhibit. Moreover, with the aim of controlling the stacking of the D−A system, the preparation of LB films[51] of bisdodecyl-substituted derivative, as well as their possible rectifying behavior, is also under study.

In addition, we have obtained a purely mixed-valence compound $\mathbf{9}^{-\bullet}$ in which the existence of a temperature-dependent intramolecular electron transfer has clearly been established. The results we have just presented unambiguously show that TTF is a suitable bridge for promoting intramolecular electron transfer between two redox centers. Such a system is of particular interest for understanding electron-transfer processes for the design of molecular wires.[52]

## Experimental Section

The general procedure is listed in Supporting Information. The melting points are uncorrected. $^1$H NMR (200 or 500 MHz) spectra were measured with $Me_4Si$ as an internal standard; the $\delta$ and $J$ values are given in parts per million and hertz, respectively. The IR spectra are recorded in units of $cm^{-1}$.

**2,5-Dihydroxyphenyl-1-piperidinedithioate 11.** To a solution of *p*-benzoquinone (5.40 g, 50 mmol) in a solution of glacial acetic acid (24 mL) and DMF (24 mL) was added rapidly at 0 °C a solution of the dithiocarbamate salt (12.2 g, 50 mmol) in a mixture of DMSO (12 mL) and DMF (24 mL). The mixture was stirred for 1 h before dilution with 500 mL of water. Filtration of the precipitate yielded 13 g (yield = 97%) of white crystals. Mp = 94−96 °C.

**4,7-Dihydroxy-1,3-benzodithioyliden-2-*N*-piperidinium Acetate 12.** *p*-Benzoquinone (5.22 g, 48 mmol) was added to a solution of compound **11** (13 g, 48 mmol) dissolved in 250 mL of methanol, immediately yielding a red precipitate. The mixture was stirred for an additional 30 min and then filtered. The precipitate was washed with methanol and then dissolved in 20 mL of glacial acetic acid, and the solution was heated for 10 min at 80 °C. After the mixture was cooled, the addition of 150 mL of acetone afforded after filtration 15.16 g (yield = 96%) of pale gray crystals. Mp = 152−154 °C.

**4,7-Dihydroxy-1,3-benzodithiole-2-thione 13.** To a suspension of the iminium salt **12** (9.80 g, 31 mmol) in 130 mL of methanol was added by fractions sodium sulfide nonahydrate (59.3 g, 0.246 mol) with vigorous stirring. After stirring at room temperature for 3 h, the red solution was poured into a mixture of glacial acetic acid (80 mL) and water (2 L). The solution was stored in a refridgerator for 48 h, and then filtration yielded 6.67 g (yield = 98%) of pale yellow crystals. Mp = 239 °C (AcOH/MeOH) (lit.[19a] 238 °C).

**4,7-Diacetyloxy-1,3-benzodithiole-2-thione 14a.** To a suspension of hydroquinone **13** (7.12 g, 33 mmol) in 30 mL of $CH_2Cl_2$ were successively added 37 mL of triethylamine (0.263 mol) and 12.4 mL (0.132 mol) of acetic anhydride. After stirring for 1 h, the mixture was partially concentrated. After addition of 50 mL of petroleum ether, the precipitate was filtered and washed with methanol, affording 7.9 g (yield = 80%) of yellow crystals. Mp = 154 °C ($CH_2Cl_2$) (lit.[19a] 148−149 °C).

**4,7-Bis(*tert*-butyldiphenylsilyloxy)-1,3-benzodithiole-2-thione 14b.** To a solution of hydroquinone **13** (6.48 g, 30 mmol) in 120 mL of DMF were successively added *tert*-butyldiphenylchlorosilane (20.4 mL, 78 mmol) and imidazole (10.2 g, 150 mmol). The mixture was stirred overnight at room temperature. After addition of methanol (300 mL), the precipitate was filtered, and recrystallization furnished 17.68 g (yield = 86%) of yellow crystals. Mp = 176 °C ($CH_2Cl_2$/petroleum ether). Anal. Calcd for $C_{39}H_{40}O_2S_3Si_2$ (693.10): C, 67.58; H, 5.82; S, 13.88. Found: C, 67.52; H, 5.84; S, 13.99.

**4,7-Diacetyloxy-1,3-benzodithiole-2-one 15a.** To a solution of compound **14a** (4.95 g, 16.5 mmol) in $CH_2Cl_2$ (150 mL) and glacial acetic acid (110 mL) was added mercuric acetate (13.09 g, 41.1 mmol). After stirring at room temperature for 15 min, the solution was filtered on Celite. The solution was successively washed with water (3 × 150 mL), a saturated solution of $NaHCO_3$ (4 × 50 mL), and water (50 mL). The organic layer was dried ($MgSO_4$) and concentrated. The residue was purified by chromatography on silica gel ($CH_2Cl_2$). Recrystallization using $CH_2Cl_2$/petroleum ether afforded 4.10 g of white crystals (yield = 88%). Mp = 164 °C (lit.[19a] 163−164 °C).

**4,7-Bis(*tert*-butyldiphenylsilyloxy)-1,3-benzodithiole-2-one 15b.** The same experimental procedure that afforded **15a** was followed, starting from 2.68 g (8.9 mmol) of compound **14b**. The residue was purified by chromatography on silica gel ($CH_2Cl_2$/petroleum ether = 1/4). Recrystallization using $CH_2Cl_2$/petroleum afforded 2.16 g of white crystals (yield = 85%). Mp = 180 °C. Anal. Calcd for $C_{39}H_{40}O_3S_2Si_2$ (676.20): C, 69.19; H, 5.96; S, 9.47. Found: C, 69.08; H, 5.98; S, 9.77.

**Bis(1,4-diacetyloxy)dibenzotetrathiafulvalene 16.** A solution of 9.94 g of compound **15a** (35 mmol) in freshly distilled triethyl phosphite (75 mL) was refluxed for 3 h and 30 min. After the solution was cooled, the precipitate was filtered and the yellow crystals were washed with methanol (4.20 g; yield = 45%); mp > 280 °C (lit.[19a] > 280 °C).

**2,3-Bis(pentylsulfanyl)-6,7-[3,6-bis(*tert*-butyldiphenylsilyloxy)benzo]tetrathiafulvalene 18.** To a solution of 0.62 g (1.5 mmol) of phosphonate **17** in 15 mL of anhydrous THF was added, under an inert atmosphere at −78 °C, 1.0 mL (1.6 mmol) of *n*-BuLi (1.6 M in hexane). After the solution was stirred for 10 min, a solution of dithiolone **15b** (0.51 g, 0.75 mmol, 1 equiv) in 15 mL of anhydrous THF was added dropwise. After stirring for 3 h at room temperature, the reaction mixture was concentrated and purified by chromatography on silica gel ($CH_2Cl_2$/petroleum ether 1/9 to eliminate impurities and then 1/4 for the elution of compound **18**) affording 0.65 g of yellow crystals (yield = 90%); mp = 104 °C ($CH_2Cl_2$/petroleum ether); MS *m*/*z* (I%) 966 ($M^{+\bullet}$, 100), 864 (8), 534 (9), 457 (26), 135 (15).

**(2,3)-(6,7)-Bis(1,4-dioxo-1,4-dihydrobenzo)tetrathiafulvalene 9.** To a solution of 106 mg (0.224 mmol) of TTF derivative **16** in 15 mL on anhydrous THF was added a sodium methanolate solution prepared by treatment of 50 mg (2.24 mmol) of sodium in 3 mL of anhydrous methanol. The green

(50) For a review on TCNQ and DCNQI electron acceptors, see: Martín, N.; Segura, J. L.; Seoane, C. *J. Mater. Chem.* **1997**, *7*, 1661.
(51) Nadizadeh, H.; Mattern, D. L.; Singleton, J.; Wu, X.; Metzger, R. M. *Chem. Mater.* **1994**, *6*, 268.
(52) (a) Creager, S.; Yu, C. J.; Bamdad, C.; O'Connor, S.; MacLean, T.; Lam, E.; Chong, Y.; Olsen, G. T.; Luo, J.; Gozin, M.; Kayyem, J. F. *J. Am. Chem. Soc.* **1999**, *121*, 1059. (b) Caroll, R. L.; Gorman, C. B. *Angew. Chem., Int. Ed.* **2003**, *41*, 4378.

solution was stirred for 1 h at 60 °C, and then acidified by addition of 426 mg (2.24 mmol) of *p*-toluenesulfonic acid monohydrate. After the solution was stirred for 5 min, 107 mg of DDQ (0.471 mmol) was added and the solution was stirred for 2 h at room temperature. After dilution with $CH_2Cl_2$, the organic layer was washed with brine, dried ($MgSO_4$), and concentrated in vacuo. The purification on florisil (100−200 mesh) column chromatography using $CH_2Cl_2$/EtOAc (99/1) as a mixture of eluents followed by a recystallization in $CH_2Cl_2$/petroleum ether afforded 46 mg of blue crystals (yield = 57%): thermal gravimetric analysis (TGA) 240 °C (dec.); IR(KBr) $cm^{-1}$ 1656 (C═O), 1544 (C═C); MS *m*/*z* (I%) 364 ($M^{+\bullet}$, 100), 226 (67), 88 (44).

**Crystallographic Data of Compound 9.** Single crystals of (0.5 × 0.13 × 0.05 mm) were grown at 293 K by slow evaporation of a $CH_2Cl_2$/petroleum ether solution containing **9**: $C_{15}H_6Cl_2O_4S_4$, M = 449.34 g/mol; monoclinic, *P*21/*c*; $a$ = 5.829(1), $b$ = 10.355(2), $c$ = 14.429(3) Å, $\beta$ = 98.19(2)°, $V$ = 862.0(3) $Å^3$, $Z$ = 2, $\rho_{calcd}$ = 1.731 $g/cm^3$, $\lambda$(Mo Kα) = 0.71073 Å, 6445 reflections ($2 < \theta < 25°$) were collected at 293 K, 1626 unique reflections and 842 reflections with $I > 2\sigma(I)$ used in refinements, 129 parameters, $R$ = 0.0537, w$R$ = 0.0885. **Cation Radical $9^{+\bullet}\cdot CF_3SO_3^-$.** To a solution of 46.7 mg (0.128 mmol) of Q−TTF−Q **9** in 1.5 mL of $CH_3CN$ was added 20.61 mg (0.064 mmol) of iodobenzene diacetate $PhI(OAc)_2$ and then 22.4 μL (0.256 mmol) of trifluoromethanesulfonic acid. After the mixture was stirred for 1 h, the resultant black precipitate was filtered and washed with diethyl ether (10 mL), toluene (10 mL), and $CH_2Cl_2$ (10 mL) successively. The black precipitate (36 mg) was isolated in 55% yield: IR (KBr) $cm^{-1}$ 1658 (C═O), 1255, 1027, 636 ($SO_3^-$). Anal. Calcd for $C_{15}H_4F_3O_7S_5$ (514.52): C, 35.02; H, 0.98; S, 31.16. Found: C, 34.88; H, 1.08; S, 31.39.

**Anion Radical $9^{-\bullet}\cdot P(C_6H_5)_4^+$.** Q−TTF−Q **9** (5 mg) was dissolved in 2 mL of a 0.2 M solution of tetraphenylphosphonium bromide in anhydrous $CH_2Cl_2$. A Cu wire was introduced and led to react at room temperature for 24 h. After removal of Cu wire, the reaction mixture was centrifuged and the precipitate washed with $CH_2Cl_2$ several times, giving 6 mg of greenish powder (62% yield): IR (KBr) $cm^{-1}$; 1633, 1615 (C═O), 760, 723, 691 (P−C). UV−vis (ethyl acetate) $\lambda$ (nm) 421, 516. Anal. Calcd for $C_{38}H_{24}O_4PS_6$ (703.84): C, 64.85; H, 3.44; S, 18.22. Found: C, 65.11; H, 3.00; S, 17.72.

**2,3-Bis(pentylsulfanyl)-6,7-(1,4-dioxo-1,4-dihydrobenzo)tetrathiafulvalene 10a.** To a solution of 100 mg (0.1 mmol) of TTF **18** in 8 mL of anhydrous THF was added 0.26 mL (0.26 mmol) of *n*-$Bu_4NF$ (1 M in THF). After the solution was stirred for 30 min at room temperature, 112 mg (0.14 mmol) of *p*-benzoquinone was added, and stirring was continued for an additional 5 min. The purification on florisil (100−200 mesh) column chromatography using $CH_2Cl_2$/petroleum ether (1/1) followed by a recystallization in $CH_2Cl_2$/petroleum ether afforded 38 mg of green crystals (yield = 75%): thermal gravimetric analysis (TGA) 290 °C dec.; IR (KBr) $cm^{-1}$ 1650; MS *m*/*z* (I%) 488 ($M^{+\bullet}$, 100), 384 (13), 347 (12), 259 (10), 226 (22). Anal. Calcd for $C_{20}H_{24}O_2S_6$ (488.77): C, 49.15; H, 4.95; S, 39.36. Found: C, 49.11; H, 5.00; S, 37.92.

**4,9-Dioxo-4,9-dihydronaphtho[2,3-*d*]-1,3-dithiole-2-one 19.** To a suspension of 16.75 g of finely powdered $K_2S$ (152 mmol) in 40 mL of DMF was added 7.5 mL (125 mmol) of $CS_2$. After the mixture was stirred for 2 h at room temperature, 14.2 g (62.5 mmol) of 2,3-dichloronaphthoquinone was added. After stirring for 30 min, the reaction mixture was diluted with dichloromethane, washed with water, and dried ($MgSO_4$), and the solvents were partially concentrated. The product was precipitated by addition of methanol, and 10.7 g of red crystals was isolated (yield = 65%): mp = 164 °C ($CH_2Cl_2$) (lit.[16a] 160−162 °C); MS *m*/*z* (I%) 264 ($M^{+\bullet}$, 100), 188 (38), 160 (12), 132 (10), 104 (43), 76 (30).

**4,9-Dihydroxynaphtho[2,3-*d*]-1,3-dithiole-2-one 20.** A solution of 5 g (18.9 mmol) of compound **19** was shaken in a separating funnel in 200 mL of an aqueous solution of sodium dithionite ($Na_2S_2O_4$) (4% w/w). The initial red solution became yellow, and the organic layer was washed with water, dried ($MgSO_4$), and then concentrated to afford 3.80 g of yellow powder (yield = 75%); mp = 222−224 °C ($CH_2Cl_2$) (lit.[16a] 222−224 °C).

**4,9-Diacetyloxynaphtho[2,3-*d*]-1,3-dithiole-2-thione 21.** To a suspension of 3.8 g (14.3 mmol) of compound **20** in 40 mL $CH_2Cl_2$ were successively added 17 mL of triethylamine (121 mmol) and 6 mL (60.5 mmol) of acetic anhydride. After the mixture was stirred for 1 h, the yellow precipitate was filtered and 3.92 g of yellow crystals was obtained (yield = 79%); mp = 240 °C ($CH_2Cl_2$).

**4,9-Diacetyloxynaphtho[2,3-*d*]-1,3-dithiole-2-one 22.** To a solution of 3.92 g (11.2 mmol) of compound **21** in 100 mL of $CH_2Cl_2$ and 80 mL of glacial acetic acid was added 9.08 g (28.5 mmol) of mercuric acetate. After stirring for 15 min at room temperature, the reaction mixture was filtered on Celite. The filtrate was successively washed with water (2 × 100 mL), a saturated aqueous $NaHCO_3$ solution (2 × 100 mL), and then water (50 mL). The organic layer was dried ($MgSO_4$), and the solvent was concentrated to afford 3.6 g of white crystals (yield = 96%).

**Bis(1,4-diacetyloxynaphtho)tetrathiafulvalene 23.** A solution of 3.6 g (10.8 mmol) of compound **4** in 25 mL of freshly distilled triethyl phosphite was refluxed for 1 h. After the solution was cooled, the precipitate was filtered and washed with methanol to afford 2 g of yellow crystals (yield = 53%): mp > 300 °C; MS *m*/*z* (I%) 636 ($M^{+\bullet}$, 100), 622 (17), 600 (30), 558 (15), 506 (25).

**(2,3)-(6,7)-Bis(1,4-naphthoquinone)tetrathiafulvalene 8.** To a suspension of 200 mg (0.31 mmol) of compound **23** in 25 mL of anhydrous THF was added a solution of 170 mg (3.14 mmol) of sodium methoxide in 5 mL of anhydrous methanol. The green suspension was heated for 4 h at 80 °C. After the suspension was cooled at 0 °C, 597 mg of *p*-toluenesulfonic acid monohydrate (3.14 mmol) and 148 mg (0.65 mmol) of DDQ were added. After the mixture was stirred for an additional 2 h at room temperature, the precipitate was filtered, washed with THF to afford 100 mg of green crystals (yield = 68%): mp > 300 °C; MS *m*/*z* (I%) MALDI 464 ($M^{+\bullet}$); IR (KBr) $cm^{-1}$ 1654 (C═O).

**Acknowledgment.** This work was partially supported by grants from the MENRT for Nicolas Gautier, the "Ville d'Angers" for Frédéric Dumur, DGI-Spain BQU2000-1157, and DURSI-Catalunya 2001SGR-00362. This research was undertaken as part of the European collaborative COST Program (Action D14/0004/99).

**Supporting Information Available:** $^1H$ and $^{13}C$ NMR and IR data with assignment of all signals; $^1H$ and $^{13}C$ NMR spectra of dyad **10a**; IR spectra of triad **9** and cation radical $9^{+\bullet}\cdot CF_3SO_3^-$ in KBr pellets; ESR spectrum of cation radical $9^{+\bullet}\cdot CF_3SO_3^-$ in acetone solution; IR spectrum of anion radical $9^{-\bullet}\cdot P(C_6H_5)_4^+$ in KBr pellets; ESR spectrum of the solid $9^{-\bullet}\cdot P(C_6H_5)_4^+$ in ethyl acetate at 300 K; evolution of the UV−vis−NIR spectrum at the beginning of the reduction of A−D−A **9**; and crystallographic data for triad **9**. This material is available free of charge via the Internet at http://pubs.acs.org.

JO035689F